Colloids and Surfaces A: Physicochem. Eng. Aspects 508 (2016) 21–29

Contents lists available at ScienceDirect

Colloids and Surfaces A: Physicochemical and Engineering Aspects

journal homepage: www.elsevier.com/locate/colsurfa

Factors affecting the coalescence stability of microbubbles

N. Pagureva [a], S. Tcholakova [a,*], K. Rusanova [a], N. Denkov [a], T. Dimitrova [b]

[a] Department of Chemical and Pharmaceutical Engineering, Faculty of Chemistry and Pharmacy, University of Sofia, 1 James Bourchier Ave., 1164 Sofia, Bulgaria
[b] DOW Corning Europe SA, Rue Jules Bordet, Parc Industriel Zone C, 7180 Seneffe, Belgium

HIGHLIGHTS

- The coalescence stability of bubbles with size from 300 to 2000 μm is studied.
- The larger bubbles coalesce for less than 50 s.
- The smallest bubbles remain stable for more than 900 s.
- The bigger bubbles form thinner foam films due to water evaporation.
- Increasing the relative humidity increases the stability of large bubbles.

GRAPHICAL ABSTRACT

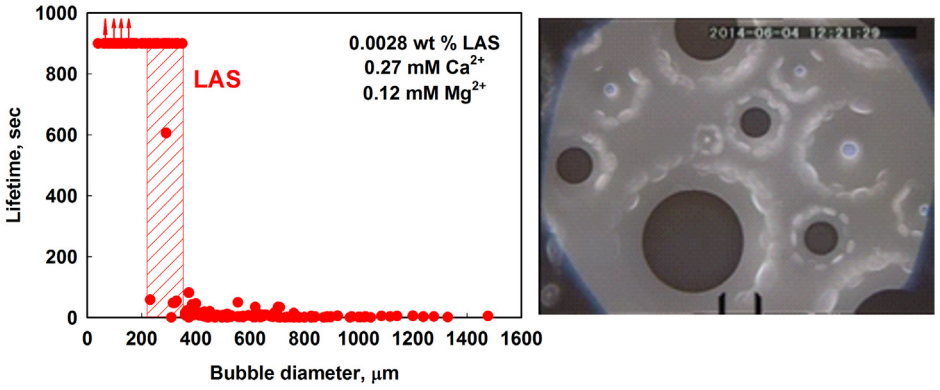

ARTICLE INFO

Article history:
Received 21 June 2016
Received in revised form 11 August 2016
Accepted 13 August 2016
Available online 13 August 2016

Keywords:
Microbubbles
Foam films
Bubble coalescence
Foam stability
Film thickness

ABSTRACT

Systematic experiments are performed to determine the factors affecting the coalescence stability of microbubbles, attached to an air-water interface. We studied the effects of bubble size, surfactant concentration, presence of co-surfactants, and relative humidity of the ambient atmosphere on the lifetime of microbubbles, with diameter varied between 300 and 2000 μm. The obtained results show that the bubble lifetime depends significantly on the bubble size, when the surfactant concentration is around or below the critical micellization concentration (CMC). Bubbles with diameter below 500 μm may have a lifetime longer than 15 min, while the bubbles with diameter above 1000 μm live for less than 10 s, under otherwise equivalent conditions. The stability of bubbles with intermediate size exhibits stochastic characteristics – some bubbles are stable for more than 15 min, whereas others coalesce for less than 1 min. This significant effect of the bubble size on the bubble lifetime is explained with the different compressing pressures, squeezing the foam film surfaces, for big and for small bubbles. The effect of water evaporation from the foam films is particularly important in these systems, as it leads to much thinner and less stable foam films for the bigger bubbles. Concomitantly, the increase of the relative humidity of the ambient atmosphere leads to larger film thickness and higher stability. These effects are important when analyzing the stability of foams, containing bubbles with different sizes, and used in atmosphere with variable relative humidity.

1. Introduction

Revealing the factors which can be used to control the formation and stability of foams is of crucial importance for various industries,

* Corresponding author.
E-mail addresses: SC@LCPE.UNI-SOFIA.BG, sc@dce.uni-sofia.bg (S. Tcholakova).

http://dx.doi.org/10.1016/j.colsurfa.2016.08.012
0927-7757/

in which the foams are used as product or formed during product application, such as food and beverages, home and personal care products, flotation, paper making, etc. The requirements for foam lifetime depend significantly on the specific application. It varies from months for aerated food products to minutes for home and personal care products [1,2]. In some cases the formation of stable foam is very undesirable and antifoams are used to prevent the foam formation or to destroy it after a certain period of time [3–5]. In the recent years there is an increasing interest to understand the factors affecting the long-term stability (days and years) of microbubbles with respect to Ostwald ripening, which is important for aerated food products and ultrasound contrasting agents for imaging [6–10]. However, from the viewpoint of home and personal care product applications and froth flotation industry, the short-term stability of bubbles within minutes, which is usually determined by bubble coalescence stability, is of major interest.

Due to its practical importance, the coalescence stability of foams was extensively studied in the literature for many years [11–20]. In the course of these studies it was found that there is a critical capillary pressure, above which the foams become unstable [11,12], as well as the existence of threshold air volume fraction, above which the rate of bubble coalescence dramatically increases [13]. In a recent study [19] it was shown that, in foams subject to perturbations and bubble rearrangement (T1 events), the coalescence occurs when the available liquid in the Plateau borders and nodes is too small for formation of stable transient foam films in the process of bubble rearrangements. These processes are relevant for foams with high air volume fraction, when relatively high surfactant concentrations are used for bubble stabilization.

For foams formed from solutions with relatively low surfactant concentration, around or below the CMC, the coalescence between bubbles is very pronounced even at low air volume fraction and have to be taken into account when analyzing the foamability of such solutions. In several recent papers Ghosh et al. [16,17,21,22] studied the bubble stability at different surfactant concentrations, for various surfactants and surfactant mixtures. It was shown that the coalescence time has stochastic distribution for all studied surfactants. Good agreement was established between the coalescence time and the foamability of the surfactant solutions studied [16,17], which shows that the lifetime of individual bubbles can be used to predict the stability of real foams. However, in most of these studies the bubbles with relatively large size were used, around 2.5 mm.

On the other hand, it is known in literature that the bubble coalescence stability can depend significantly on the foam film size [20,23–26]. In the study of Gurkov et al. [23] the stability of foam films stabilized by surfactants at low concentrations was studied. It was shown that the film lifetime increases with the film radius, due to the increasing drainage time of the foam films with the increase of the film radius [23]. In contrast, it was shown by Khristov et al. [26] that the critical capillary pressure, required for foam film rupture, decreases with increasing the film radius from 0.2 to 2 mm for SDS stabilized foam films. In both studies, foam films in capillary cell are investigated.

To clarify further the effect of the film/bubble size on the bubble coalescence stability, in the current study we investigate the effects of bubble size, surfactant concentration, and presence of nonionic co-surfactants on the coalescence stability of bubbles attached to large air-water interface. Comparative experiments, aimed at determining the stability of foam films in capillary cell, were also performed. The obtained results are analyzed and a significant effect of the relative humidity of the ambient atmosphere on the film and bubble stability was revealed and used to explain the experimental results.

2. Materials and methods

2.1. Materials

As main surfactant we used linear alkyl benzene sulfonate, LAS (product of Dow Corning, purity 53,7%, LOT: 25313-30-3) and as co-surfactants we used two different nonionic surfactants NI (product of Dow Corning, LOT: 25313-30-4) and Polyoxyetylene-7 C12/15 ether (trade name Neodol 25-7, product of Shell) denoted as EO7 in the text. To vary the ionic strength we used $CaCl_2$ (product of Chem-Lab, CL00.0317.1000) and magnesium dichloride $MgCl_2$ (product of Valerus, Cat N 2265). All solutions contain Ca^{2+} and Mg^{2+} at 9:4 molar ratio and were prepared with deionized water from Elix purification system.

Three stock solutions were prepared: (1) 6 g/L LAS, (2) 27 mM $CaCl_2$ + 12 mM $MgCl_2$, and (3) 0.6 g/L nonionic surfactant NI. In some of the experiments NI in the mixtures was replaced by EO7. The stock solution of 0.6 g/L NI surfactant was prepared by melting the surfactant at 50 °C and mixing it with pre-heated water at 50 °C for 1 h. Working solutions were prepared by mixing the three stock solutions at appropriate ratios. In the mixtures LAS + NI (denoted as LNI) and LAS + EO7 (denoted as LEO) the ratio between LAS and nonionic surfactant is 8.3:1 wt:wt.

2.2. Measurement of the surface tension of the solutions

The equilibrium surface tension of the foaming solutions, σ, was measured with Wilhelmy plate method on tensiometer K100 (Kruss GmbH, Germany).

2.3. Procedure for bubble formation

Bubbles were generated via vigorously mixing of 300 mL of working solution in a vessel with volume of 600 mL for 2 min at maximum speed with Silverson AG1-10727. After that the generated bubbles were collected with syringe equipped with needle and put in a vessel with solution, which is equipped with Teflon coverage to ensure a convex meniscus and therefore the bubbles are positioned in the center of the meniscus. They stayed on the meniscus which allows us to measure their size and to determine their stability. As a measure of bubble stability we used bubble lifetime which was defined as a time in which bubble is stable after placing it in the petri dish.

2.4. Optical observations of foam films and bubbles

Optical observations of the studied systems were performed in reflected or transmitted monochromatic light, by means of a microscope Axioplan (Zeiss, Germany), equipped with a long-distance objectives: Plan-Neofluar 2.5×/0.075; Plan-Neofluar 10×/0.3; Zeiss Epiplan 20×/0.40; Zeiss Epiplan 50×/0.50, CCD camera, video-recorder and monitor. The bubble equatorial diameter was measured in transmitted light, whereas the thickness of the film formed between bubbles and large air-water interface was determined in reflected light. Depending on the film thickness, the light reflected by the film has different colours. From the colour and from the intensity of the light reflected from the foam film, one could determine the film thickness with rather good precision [27]. The films that are thicker than 100 nm appear colored. The films with thickness of about 100 nm appear white (bright), those with thickness of about 50 nm appear grey, and those which thickness is under 30 nm appear dark. All of the experiments were conducted at ambient temperature (25 °C).

2.5. Observation of foam films in a capillary cell

Foam films of millimeter size were formed and observed in a capillary cell to obtain information for the dynamics of thinning of the films and the equilibrium film thickness. The observations were made by using Scheludko method [27]. The films were formed from a biconcave drop, placed in a short capillary (i.d. 2.5 mm, height 3 mm), by sucking out liquid through a side orifice. The observations were performed in reflected monochromatic light, by means of a microscope Axioplan (Zeiss, Germany), equipped with a long-distance objective Zeiss Epiplan 20×/0.40, CCD camera, video-recorder and monitor.

2.6. Measurement of the surface rheological properties of the solutions

The surface dilatational modulus of the surfactant solutions was measured by the oscillating drop method on DSA10 instrument, equipped with ODM/EDM module (Krüss, Germany) [28]. The principle of the method is the following: By using a piezo-driven membrane, small oscillations are generated in the volume of a pendant drop (hanged on a needle tip). These oscillations lead to periodical expansions/contractions of the drop surface area: $a(t) = a_0 \sin(\omega t)$, where $a(t) = [A(t) - A_0]/A_0$ is the normalized change of the surface area around the mean area, A_0, while a_0 is the relative amplitude of oscillations and $\nu = 2\pi\omega$ is the frequency of oscillations. Video-images of the oscillating drop are recorded and analysed by the Laplace equation of capillarity in order to determine the variation of the surface tension, σ, with time. For small deformations, the variation of the surface tension is harmonic:

$$\sigma(t) = E' a_0 \sin(\omega t) + E'' a_0 \cos(\omega t) \quad (1)$$

where E' is the surface elastic modulus (related to surface elasticity) and E'' is the surface viscous modulus (related to surface dilatational viscosity, $\mu_{SD} = E''/\omega$). The total surface dilatational modulus is:

$$E_D = \left((E')^2 + (E'')^2 \right)^{1/2} \quad (2)$$

In the experiments performed in the current study the relative area amplitude was in the range ≈2 ÷ 4%, and the period of deformation was varied in the range 2 ÷ 10 s. The temperature was kept constant, $T = 25\,^{\circ}C$, via a thermostating chamber TA10 (Krüss, Germany).

3. Experimental results and discussion

3.1. Surface properties of studied surfactant systems

In Fig. S1 in Supporting information we show illustrative original data for the surface tension, as a function of time, along with the best fit to the same data by the dependence surface tension vs. the inverse square root of time. From this fit we determined the equilibrium surface tension at given surfactant concentration. These data are used to construct the adsorption isotherms for studied surfactant solutions, shown in Fig. 1. The addition of nonionic surfactants to the solution of LAS leads to a significant decrease of the surface tension at surfactant concentrations below the CMC, and to significant decrease of the CMC values, which means that a mixed adsorption layer is formed on the solution surface [29–31].

From the dependence of the surface tension on surfactant concentration we determined the surfactant adsorption at CMC using Gibbs adsorption isotherm [32–34]:

$$\frac{d\sigma}{d \ln C_S} = -k_B T \Gamma \quad (3)$$

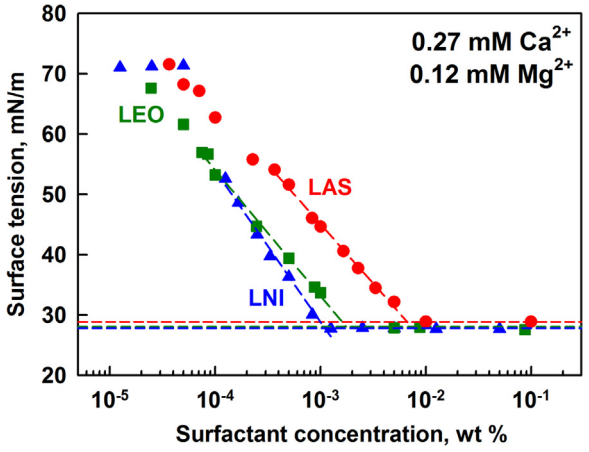

Fig. 1. Surface tension isotherms for the surfactant systems studied: LAS (red circles), LEO (green squares), LNI (blue triangles), in presence of 0.27 mM Ca^{2+} and 0.12 mM Mg^{2+}. (For interpretation of the references to colour in this figure legend, the reader is referred to the web version of this article.)

Table 1
Critical micellar concentration, surface tension at CMC, surfactant adsorption at CMC, Γ_{CMC} and area per molecule in the surfactant adsorption layer at CMC, A_{CMC}, for layers formed from the different solutions in the presence of 0.27 mM Ca^{2+} and 0.12 mM Mg^{2+}. The values for Γ_{CMC} and A_{CMC} of the mixed solutions correspond to the total surfactant adsorption, which is calculated in a straightforward manner from an analogue of Eq. (3), including the contributions of the two surfactants in the Gibbs isotherm.

System	CMC, wt%	σ_{CMC}, mN/m	Γ_{CMC}, μmol/m²	A_{CMC}, nm²
LAS	6.7×10^{-3}	28.9 ± 0.2	3.8 ± 0.1	0.44 ± 0.02
LAS + EO7	1.8×10^{-3}	28 ± 0.2	4.0 ± 0.1	0.42 ± 0.02
LAS + NI	1×10^{-3}	27.8 ± 0.2	4.8 ± 0.1	0.35 ± 0.02

where k_B is Boltzmann constant, T is temperature, Γ is adsorption, σ is surface tension and C_S is bulk surfactant concentration. We assumed that the variation of Na^+ ions with the variation of surfactant concentration has no significant impact on the adsorption, as far as the present Ca^{2+} ions are prevailing in the adsorption layer of LAS [35]. The obtained results for the three surfactant mixtures studied are shown in Table 1.

The surfactant adsorption for LAS molecules in the absence of nonionic surfactant is 3.8 μmol/m², which corresponds to 0.44 nm² area per molecule in the adsorption layer. This result is in a good agreement with the data obtained by Anachkov et al. [35]. The addition of nonionic surfactant in the solution increases the adsorption from 3.8 μmol/m² to 4.0 μmol/m² for LAS + EO7 and to 4.8 μmol/m² for LAS + NI. The higher value for NI is most probably related to the longer chain length of this nonionic surfactant, as compared to EO7.

Along with the higher surfactant adsorption, the addition of nonionic surfactant leads to lower CMC. The effect is more pronounced for NI as compared to EO7, which is again attributed to the longer chain length of NI. For further experiments we choose three concentrations around the CMC for the solutions studied: 0.0014 wt%, 0.0028 wt%, and 0.0056 wt%. The lowest surfactant concentration is very close to CMC for LAS + NI mixture, the intermediate concentration is close to CMC for LAS + EO7 mixture, and the highest concentration is around CMC for LAS solution. Therefore, the studied concentrations are above CMC for LAS + NI, below CMC for LAS, and above and below CMC for LAS + EO7. The main series of experiments is performed with 0.0028 wt% surfactant solutions.

To characterize the rheological properties of the formed adsorption layers we measured their surface moduli, as a function of surface oscillation frequency. The experimental results are shown

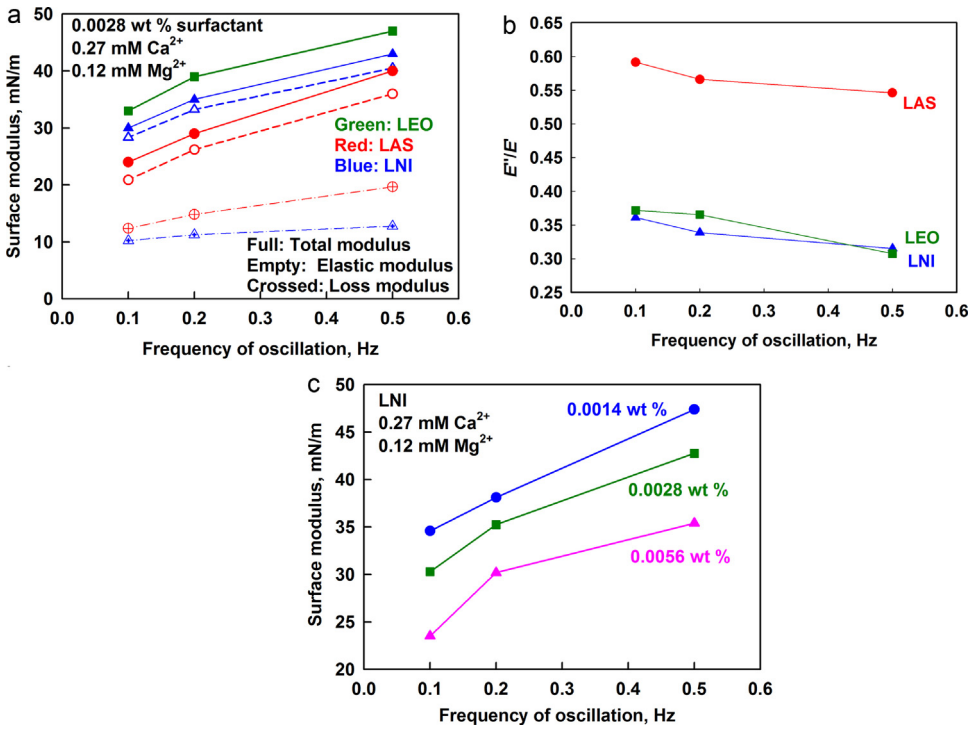

Fig. 2. (A) Total (full symbols); elastic (empty symbols) and viscous (crossed symbols) as a function of frequency of oscillation for LNI (blue triangles), LEO (green squares), LAS (red circles); (B) Ratio between viscous and elastic modulus for data shown in (A) and (C) Total surface modulus for surface layers formed from LAS + NI solutions at three different surfactant concentrations as indicated in the figure. All experimental data are obtained from solutions which contain 0.27 mM Ca^{2+} and 0.12 mM Mg^{2+}. (For interpretation of the references to colour in this figure legend, the reader is referred to the web version of this article.)

in Fig. 2. For all surfactants studied the elastic and viscous surface moduli increase with increasing the frequency of oscillation, which is typical behavior for surfactant layers formed from solutions with concentrations below and around the CMC. The surface moduli decrease with increasing the surfactant concentration, which is typical case for soluble surfactants with concentration around or above the CMC [36]. Lower surface modulus measured at higher surfactant concentration is related to the faster surfactant adsorption, which results in lower variations in surface tension upon oscillation. The adsorption layers formed from LAS solutions exhibit the lowest elastic modulus of all studied systems, which could be attributed to faster relaxation of the adsorption layers in this system, as compared to the layers containing nonionic surfactants.

From this series of experiments we can conclude that denser adsorption layer is formed from LAS + NI solution, followed by LAS + EO7 and LAS alone. The latter effect is explained with the electrostatic repulsion between the LAS molecules in the adsorption layer. The concentration of the Ca^{2+} and Mg^{2+} ions is relatively low in the solutions studied (0.27 mM Ca^{2+} and 0.12 mM Mg^{2+}) and these ions are unable to screen completely the electrostatic repulsion between the adsorbed LAS molecules which are negatively charged – see Ref. [35] for further experimental data and their analysis about the properties of LAS layers in presence of Ca^{2+} and Mg^{2+} ions. The presence of NI or EO7 in the solutions leads to formation of mixed adsorption layer with higher adsorption and higher surface dilatational modulus. The higher surface modulus of LAS + NI and LAS + EO7, as compared to LAS, is explained with the slower relaxation in the presence of nonionic co-surfactants.

Let us mention that all measured surface moduli are below 50 mN/m which means that the studied surfactants behave as typical low-molecular mass surfactants. Note that in our previous studies we found that co-surfactants which increase the surface modulus above 100 mN/m lead to peculiar foam properties, such as: lower rate of Ostwald ripening [37], higher viscous friction in foams [38], and faster bubble break-up in sheared foams [39]. At lower surface modulus ($E < 100$ mN/m), as in the systems studied here, E does not affect significantly the properties of the concentrated foams, but the surface modulus may have significant impact on the rate of film thinning and on the coalescence probability for small bubbles.

3.2. Stability of microbubbles

To characterize the stability of microbubbles we measured their lifetime using the procedure from Section 2.4. Typical experimental pictures and the respective results for the bubble lifetime, as a function of bubble diameter, are shown in Fig. 3. From these pictures one can see that the big bubbles coalesce very rapidly with the large air-water interface, whereas the small bubbles stay stable for very long periods of time. The latter trend is illustrated in Fig. 3C where the bubble lifetime is presented as a function of bubble diameter. Small bubbles have lifetime above 900 s, whereas the lifetime of big bubbles is below 50 s. Bubbles with intermediate sizes have intermediate stability of stochastic nature – some of them are very stable, while others are very unstable (see the shaded area in Fig. 3C). We classified the bubbles with size between 50 and 1050 μm in intervals with width of 100 μm, see Fig. 3D. The number of bubbles within different intervals varies between 35 and 5. To ensure relevant statistics, we grouped the large bubbles with diameter above 1000 μm in 500 μm intervals.

For the bubbles in each interval we determined the percentage of bubbles which remain stable for more than 900 s. Stable means that these bubbles do not coalesce with the large air-water interface during the entire experiment. Most of the smallest bubbles with size below 50 μm disappear within 900 s due to Ostwald ripening and, therefore, we do not include them in the data set. The obtained results for the percentage of stable bubbles in given size interval are shown in Fig. 3D. More than 80% of bubbles with diameter below

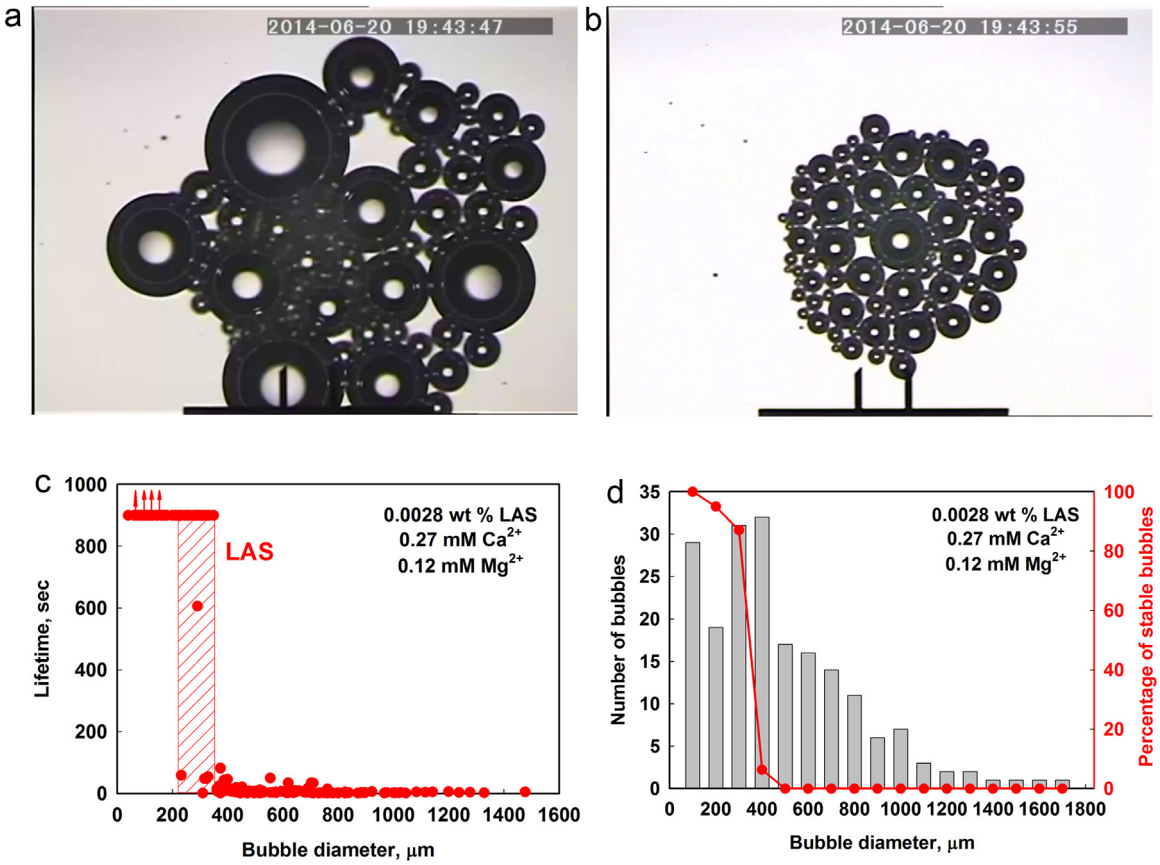

Fig. 3. (A,B) Illustrative pictures of bubble raft after placing it on the solution surface (A) and (B) 8 s later. (C) Lifetime as a function of bubble diameter for bubbles formed in LAS solution with concentration of 0.0028 wt%. (D) Number of bubbles in given interval (bars) and percentage of stable bubbles (those which do not coalesce for 900 s) within the interval (red points associated with right axis) for bubbles formed in 0.0028 wt% LAS solution in presence of 0.27 mM Ca^{2+} and 0.12 mM Mg^{2+}. The distance between the bars in (A,B) is 100 μm. (For interpretation of the references to colour in this figure legend, the reader is referred to the web version of this article.)

350 μm remain stable, whereas less than 10% of bubbles with size between 350 and 450 μm survive for more than 50 s. Therefore, the threshold bubble diameter dividing the stable from unstable bubbles is around 350 μm for the bubbles formed in LAS solution.

Comparison of the percentage of stable bubbles, as a function of their diameters, for bubbles formed in different surfactant solutions is shown in Fig. 4. For all systems studied we observed similar behavior as for LAS – the small bubbles are very stable with respect to coalescence, whereas the big bubbles above certain size become very unstable. The increase of the surfactant concentration from 0.0014 wt% to 0.0028 wt% does not affect the stability of bubbles formed in LAS and LAS + NI solution, whereas the further increase of LAS + NI concentration to 0.0056 wt% increases significantly the stability of bubbles with diameter below 1 mm. The addition of nonionic surfactants (NI or EO7) to LAS solution at both concentrations (0.0014 wt% and 0.0028 wt%) increases significantly the stability of bubbles with diameters between 400 and 600 μm.

To compare further these systems, we define the threshold bubble diameter as the diameter, at which 50% of the bubbles will remain stable for more than 900 s, whereas the other 50% coalesce within less than 50 s after foam film formation. The threshold bubble diameter is 0.4 ± 0.05 mm for bubbles formed in LAS solutions at concentrations of 0.0014 wt% and 0.0028 wt%, while it is 0.6 ± 0.05 mm for bubbles formed in LAS + NI and LAS + EO7 at the same concentration. The further increase of surfactant concentration leads to increase of the threshold bubble size up to 1 mm (Fig. 5).

From this series of experiments we conclude that the big bubbles are very unstable, while the small bubbles are very stable with respect to coalescence, when the surfactant concentration is around the CMC. The threshold bubble size, dividing the stable from unstable bubbles, depends on the surfactant concentration and the presence of nonionic co-surfactants. The threshold bubble size varies between 0.4 and 1 mm for the systems studied.

3.3. Observations of foam films

To reveal the mechanism of stabilization of the small microbubbles, we performed optical observations of the foam films, formed between the bubbles and the large air-water interface. Bubbles with diameter above 1.5 mm coalesce very rapidly with the large interface during the foam film thinning, whereas the bubbles with diameter below 1 mm are able to reach the equilibrium film thickness before their coalescence with the ambient atmosphere. Therefore, the very low stability of the big bubbles is related to the higher probability for film rupture during film thinning, due to the larger film area where the film rupture event can occur. The smaller bubbles have smaller film area and, as a consequence, they have lower coalescence probability.

Along with the smaller film area of the small bubbles, we observed that these bubbles have significantly larger film thickness under the same conditions – see the representative pictures in Fig. 6. This effect is very pronounced for the bubbles formed in LAS solution, where the change in the film thickness leads even to a transition from common black films to the much thinner Newton black films, with a significant expansion of the film area in this transition.

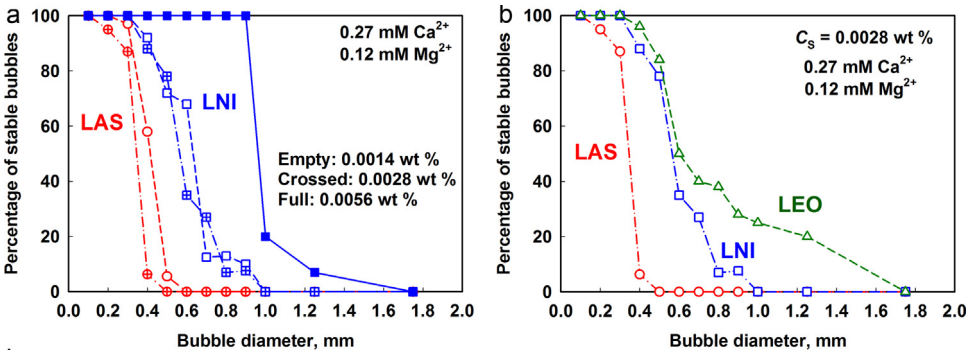

Fig. 4. Percentage of stable bubbles (those which do not coalesce for 900 s) within the interval, as a function of mean size for bubbles formed in (A) surfactant solutions with different concentrations and (B) fixed surfactant concentration for studied surfactant mixtures.

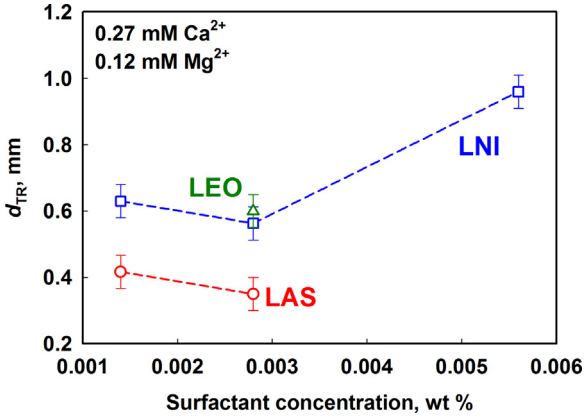

Fig. 5. Bubble size diameter dividing the stable from unstable bubbles for the various systems studied, as a function of surfactant concentration.

The latter experimental observations are explained as follows. By definition, the common black films contain an inner layer of water phase, with finite thickness (typically above 10 nm) and are stabilized by electrostatic repulsion. The van der Waals attraction in these films is not very strong and the related contact angle film-meniscus is close to zero (much less than 1°). In contrast, the Newton black films contain only a bilayer of surfactant molecules and the water molecules hydrating the surfactant head-groups. Therefore, the Newton black films are much thinner, the van der Waals attraction between the film surfaces is much stronger, and they have a significantly larger contact angle film-meniscus, typically of several degrees. The larger contact angle of the Newton black films changes the shape of the film-meniscus capillary system and a mechanical equilibrium is achieved at a larger film area (compared to common black films), under otherwise equivalent conditions.

The formation of thicker films between the small bubbles and the atmosphere is a non-trivial observation, as the compression pressure is higher for the smaller bubbles and the foam films should be thinner under equilibrium conditions. The formation of thinner films between bigger bubbles and atmosphere can be explained only if we take into account the evaporation of water from the solution surface (including the area of the foam film) during our experiments. The water evaporation from the film region is accompanied with a significant increase in the compressing pressure which squeezes the film and pushes the film surfaces against each other.

According to the model presented in Ref. [40], the compressing pressure due to water evaporation from the foam film can be estimated by the expression:

$$P_{ev} \sim \frac{\eta V_W j_e}{h^3} R_F^2 \quad (4)$$

Here j_e is the number of water molecules evaporating per unit time from unit area of the upper film surface; V_W is the volume per water molecule in the aqueous phase; h is the film thickness, η is the solution viscosity, and R_F is the film radius. For small bubbles the initial film radius is much smaller than the film radius of the bigger bubbles and, as a consequence, the compression pressure is much lower. Therefore, the small bubbles form thicker films, whereas the larger bubbles form larger films which thin down, under the action of the water evaporation and the related compressing pressure, Eq. (4). When the latter becomes sufficiently high to overcome the electrostatic barrier, a transition from common black film to Newton black film is observed. Eq. (4) shows that the compressing pressure, which is due to the water evaporation, depends also on the film thickness, which in its own turn means that the thinner films

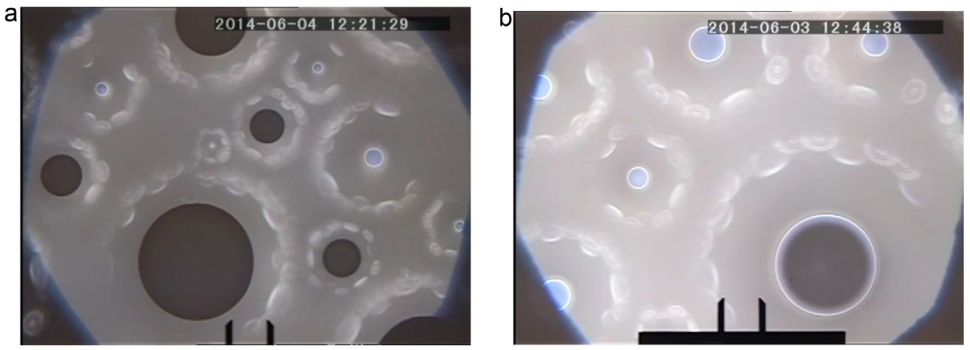

Fig. 6. Representative pictures from the foam films, formed between the ambient atmosphere and bubbles attached to the respective air-solution interface: (A) LAS solution and (B) LAS + NI solution, both with concentration of 0.0028 wt%, in presence of 0.27 mM Ca^{2+} and 0.12 mM Mg^{2+}.

with large surface area will rupture more easily. In other words, for the big bubbles, the rate of water influx from the meniscus region is slower as compared to the water evaporation and the film thins down. In this thinner film the water flux from meniscus region is even more suppressed and the films become unstable after certain period of time. That is why the bigger bubbles have much lower stability as compared to the small bubbles.

The experimental observation that the bigger bubbles formed thinner films with atmosphere has been confirmed with all other systems studied – see illustrative picture in Fig. 6B. For systems containing non-ionic surfactants, however, we did not observe phase transition from common to Newton black film – both the small and big bubbles form common black films with different thicknesses. The higher stability of bubbles formed in LAS + NI and LAS + EO7 solution, as compared to the stability of bubbles formed in LAS solution, can be attributed to the fact that the Newton films, formed with intermediate in size bubbles in LAS solutions, have much smaller thickness and much larger film area, as compared to the similar in size bubbles in LAS + NI solution. As seen from Eq. (4), smaller thickness and large surface area lead to larger compressing pressure.

To check further this explanation we performed experiments in a capillary cell, where we can control the water evaporation from the film surface. Illustrative pictures from foam films, formed in closed capillary cell, when the water evaporation is suppressed and in an open capillary cell, when the evaporation is intensive, are shown in Fig. 7. One sees that the thickness of the foam films in closed and open cells is rather different, due to the different compressing pressures in these two situations. The capillary pressure in the foam films, formed in a closed cell, is rather low (≈50 Pa), while in an open cell it is much higher ($\approx 10^5$ Pa) due to the water evaporation from the film [40]. Along with the different film thickness at the same size of the film, with and without evaporation, we found that the evaporation affects significantly the film stability. All studied films are stable in closed cell, where the compressing pressure is relatively low and the film thickness is relatively large, while in opened cell evaporation occurs and the film stability depends on the used surfactant mixture and its concentration. All films formed from LAS solutions at concentration of 0.0028 wt% were stable in closed cell and rupture for less than 50 s after opening the cell, when the films become thin in their central region. Similar behavior is observed with films formed from LAS + NI at concentration of 0.0014 wt%, but the time required to thin film down to critical film thickness varies between 30 and 120 s. The increase of LAS + NI concentration to 0.0028 wt% leads to formation of very stable films, even at high compression when water evaporation takes place. The further increase of the LAS + NI concentration does not change the stability of the foam films in capillary cell.

The fact that stable films at high compressing pressure are formed at 0.0028 wt% in capillary cell, whereas a significant increase in the stability of large bubbles is observed at concentration of 0.0056 wt% can be explained in the following way. To form a foam film in the capillary cell, it requires some period of time (e.g. 30 s to several minutes) during which the surfactant adsorbs on the air-water interfaces before the actual film is formed. Therefore, in the moment of film formation, the film surfaces are already covered with an (almost) equilibrium surfactant layer. This is not the case with the surfaces of bubbles, formed in diluted surfactant solutions – the foam films in this case are generated several seconds after bubble formation. In other words, the surfactant has much shorter period of time to adsorb in the second system and, hence, the bubble stabilization is observed at higher surfactant concentration.

From this series of experiments we can conclude that thicker films are formed between small bubbles and large air-water interface, which is explained with the smaller contribution of the water evaporation from these films, as compared to its contribution for big bubbles. The effect of water evaporation is further demonstrated with experiments performed in capillary cell, where the films are thicker in closed cell (no evaporation) and thin down after opening the cell. The higher stability of intermediate sized bubbles formed in LAS + NI is in a very good agreement with higher stability of foam films formed in capillary cell from this solution under evaporation, as compared to the stability of films formed from LAS only.

3.4. Effect of humidity on foam stability

To assess the importance of the relative humidity of the ambient atmosphere on the behavior of the foam films, we performed optical observations of films stabilized with LAS + NI at 20, 40, and 100% relative humidity, see Fig. 8. One sees that the foam films formed at higher humidity (≥40%) are much thicker. This clearly shows that the thinner films for the big bubbles are related to the higher rate of water evaporation from them, as compared to the water influx from the meniscus region. We note that all optical observations presented so far were conducted at temperature 25 °C and humidity in the range of 30–40%. From the data presented in Fig. 8A one sees that, along with the thicker films formed at higher relative humidity, the stability of the intermediate in size bubbles also increases significantly, which supports our hypothesis that the higher stability of small bubbles is related to the lower compressing pressure and the smaller film area.

4. Conclusions

Systematic series of experiments, aimed at determining the coalescence stability of microbubbles, attached to a large air-water interface, is performed. The obtained results show the existence of a threshold bubble diameter, above which the bubbles coalesce with the large interface for less than 50 s, whereas the smaller bubbles remain stable for more than 900 s. The stability of the intermediate in size bubbles has stochastic characteristics – some bubbles are stable for more than 900 s, while the others coalesce for less than 50 s.

The higher stability of the small bubbles is explained with the formation of thicker foam films between the bubbles and the large air-water interface, as compared to the larger bubbles. This difference in the film thickness and stability is explained with the important role of water evaporation from the foam film surface into the ambient atmosphere. In the case of large foam films, the evaporated water from the films cannot be compensated by influx of the liquid water, sucked from the film periphery (from the Plateau region surrounding the film). The effect of water evaporation is further demonstrated with experiments performed in capillary cell, where the films are thicker in closed cell (no evaporation) and thin down after opening the cell. The change of relative humidity during the experiment leads to formation of thicker films for intermediate in size bubbles, which is accompanied with a significant increase in film stability.

The addition of nonionic surfactant to LAS solution decreases significantly the CMC, increases the elastic surface modulus, adsorption and stability of the intermediate in size bubbles, mainly by decreasing the surface area of the thin foam films, because there is no transition from common black film to Newton black film upon evaporation, as it is the case with LAS solution.

Appendix A. Supplementary data

Supplementary data associated with this article can be found, in the online version, at http://dx.doi.org/10.1016/j.colsurfa.2016.08.012.

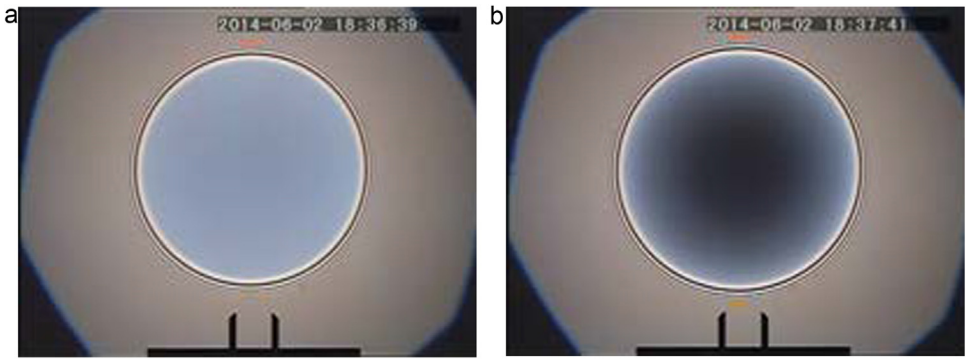

Fig. 7. Illustrative pictures of films, formed from 0.0028 wt% LAS + 0.27 mM Ca^{2+} + 0.12 mM Mg^{2+} in (A) closed capillary cell, and (B) open capillary cell just before film rupture. The distance between the bars is 50 μm.

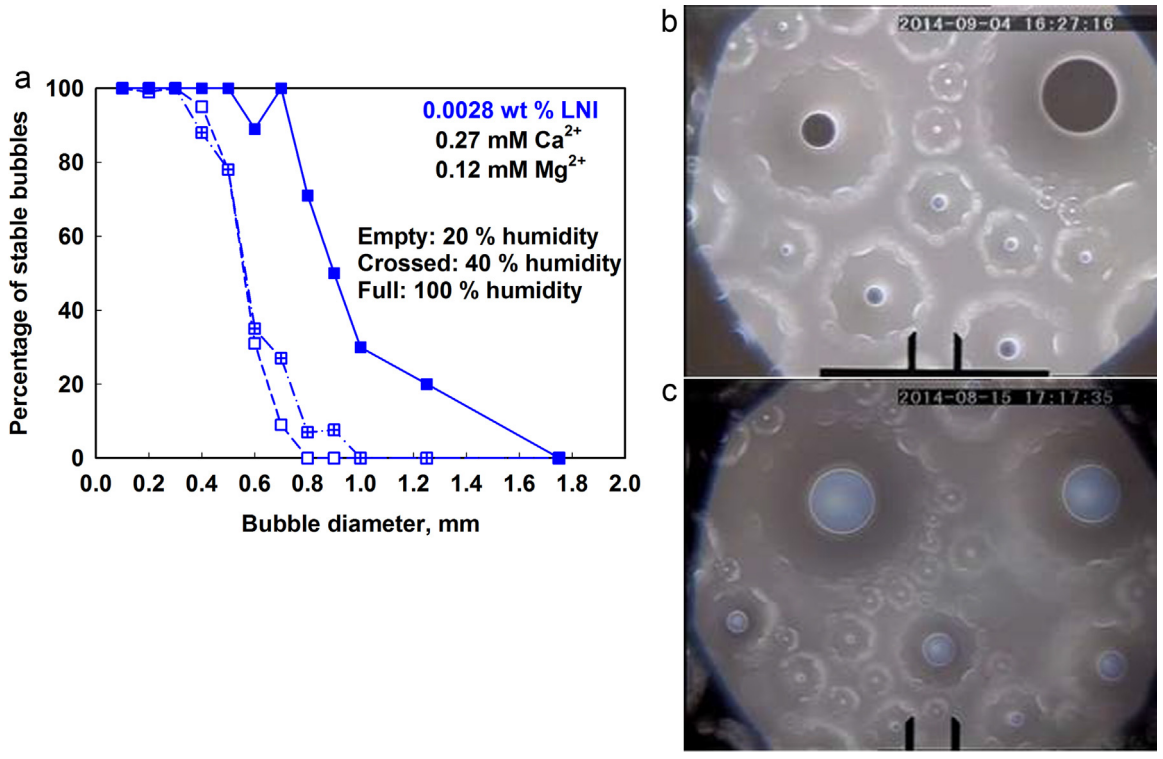

Fig. 8. (A) Percentage of stable bubbles as a function of bubble diameter as measured at three different relative humidities and illustrative pictures for the film thickness of the formed bubbles at (b) 20% and (C) 100% relative humidity. The distance between the bars is 100 μm.

References

[1] L.L. Schramm, Foams Emulsions, and Suspensions: Fundamentals and Applications, John Wiley & Sons, 2006.
[2] G. Narsimhan, E. Ruckenstein, Structure, drainage, and coalescence of foams and concentrated emulsions, in: R.K. Prud'homme, S.A. Khan (Eds.), Foams: Theory, Measurements, Applications, Surfactant Science Series, vol. 57, Marcel Dekker, New York, 1996, Chapter 2.
[3] N.D. Denkov, Langmuir 20 (2004) 9463.
[4] P. Garrett, The Science of Defoaming: Theory, Experiments and Applications, CRC, Press, Taylor & Fransis Group, 2014.
[5] N.D. Denkov, K.G. Marinova, S.S. Tcholakova, Mechanistic understanding of the modes of action of foam control agents, Adv. Colloid Interface Sci. 206 (2014) 57–67.
[6] A.B. Subramaniam, C. Mejean, M. Abkarian, H.A. Stone, Microstructure, morphology, and lifetime of armored bubbles exposed to surfactants, Langmuir 22 (2006) 5986–5990.
[7] E. Dressaire, R. Bee, D.C. Bell, A. Lips, H.A. Stone, Interfacial polygonal nanopatterning of stable microbubbles, Science 320 (2008) 1198–1201.
[8] S. Mahalingam, M.B.J. Meinders, M. Edirisinghe, Formaion, stability, and mechanical properties of bovine serum albumin stabilized air bubbles produced using coaxial electrohydrodynamic atomization, Langmuir 30 (23) (2014) 6694–6703.
[9] T.A.M. Rovers, G. Sala, E. van der Linden, M.B.J. Meinders, Temperature is key to yield and stability of BSA stabilized microbubbles, Food Hydrocoll. 52 (2016) 106–115.
[10] T.A.M. Rovers, G. Sala, E. van der Linden, M.B.J. Meinders, Effect of temperature and pressure on the stability of protein microbubbles, ACS Appl. Mater. Interfaces 8 (2016) 333–340.
[11] D. Exerowa, P.M. Kruglyakov, Foam and Foam Films, Elsevier, New York, 1998.
[12] Z.I. Khatib, G.J. Hirasaki, A.H. Falls, Effects of capillary pressure on coalescence and phase mobilities in foams flowing through porous media, SPE Reserv. Eng. 3 (1988) 919–926.
[13] V. Carrier, A. Colin, Coalescence in draining foams, Langmuir 19 (2003) 4535–4538.
[14] M.D. Eisner, S.A.K. Jeelani, L. Bernhard, E.J. Windhab, Stability of foams containing proteins: fat particles and nonionic surfactants, Chem. Eng. Sci. 62 (2007) 1974–1987.
[15] A. Bhakta, E. Ruckenstein, Decay of standing foams: drainage: coalescence and collapse, Adv. Colloid Interface Sci. 70 (1997) 1–123.
[16] P. Ghosh, Coalescence of bubbles in liquid, Bubble Sci. Eng. Technol. 1 (2009) 75–87.
[17] S. Samanta, P. Ghosh, Coalescence of bubbles and stability of foams in brij surfactant systems, Ind. Eng. Chem. Res. 50 (2011) 4484–4493.

[18] D. Langevin, E. Rio, Coalescence in foams and emulsions, in: P. Somasundaran (Ed.), Encyclopedia of Surface and Colloid and Science, 2nd ed., Taylor and Francis, New York, 2012.
[19] A.-L. Biance, A. Delbos, O. Pitois, How topological rearrangements and liquid fraction control liquid foam stability, Phys. Rev. Lett. 106 (2011) 068301.
[20] D. Langevin, Bubble coalescence in pure liquids and in surfactant solutions, Curr. Opin. Colloid Interface Sci. 20 (2015) 92–97.
[21] S. Samanta, P. Ghosh, Coalescence of bubbles and stability of foams in aqueous solutions of Tween surfactants, Chem. Eng. Res. Des. 89 (2011) 2344–2355.
[22] G. Suryanarayana, P. Ghosh, Adsorption and coalescence in mixed-surfactant systems: air-water interface, Ind. Eng. Chem. Res. 49 (2010) 1711–1724.
[23] T.D. Gurkov, J.K. Angarska, K.D. Tachev, W. Gaschler, Statistics of rupture in relation to the stability of thin liquid films with different size, Colloids Surf. A 382 (2011) 174–180.
[24] S. Tcholakova, N.D. Denkov, I.B. Ivanov, B. Campbell, Coalescence in beta-lactoglobulin-stabilized emulsions: effects of protein adsorption and drop size, Langmuir 18 (2002) 8960–8971.
[25] S. Tcholakova, N.D. Denkov, I.B. Ivanov, B. Campbell, Coalescence stability of emulsions containing globular milk proteins, Adv. Colloid Interface Sci. 123–126 (2006) 259–293.
[26] Khr. Khristov, D. Exerowa, G. Minkov, Critical capillary pressure for destruction of single foam films and foam: effect of foam film size, Colloids Surf. A 210 (2002) 159–166.
[27] A. Scheludko, Thin liquid films, Adv. Colloid Interface Sci. 1 (1967) 391.
[28] S.C. Russev, N. Alexandrov, K.G. Marinova, K. Danov, N.D. Denkov, L. Lyutov, V. Vulchev, C. Bilke-Krause, Instrument and methods for surface dilatational rheology measurements, Rev. Sci. Instrum. 79 (2008) 104102.
[29] Y. Zhu, M.J. Rosen, Synergism in binary mixtures of surfactants: IV: effectiveness of surface tension reduction, J. Colloid Interface Sci. 2 (1984) 435–442.
[30] M.F. Cox, N.F. Borys, T.P. Matson, Interactions between LAS and nonionic surfactants, JAOCS 62 (1985) 1139–1143.
[31] M.J. Rosen, Surfactants and Interfacial Phenomena, Wiley, New York, 1989.
[32] A.W. Adamson, A.P. Gast, Physical Chemistry of Surfaces, 6th ed., Wiley, New York, 1997.
[33] T.D. Gurkov, D.T. Dimitrova, K.G. Marinova, C. Bilke-Crause, C. Gerber, I.B. Ivanov, Ionic surfactants on fluid interfaces: determination of the adsorption; role of the salt and the type of the hydrophobic phase, Colloids Surf. A 261 (2005) 29–38.
[34] P.A. Kralchevsky, K.D. Danov, N.D. Denkov, Chemical physics of colloid systems and interfaces, in: K.S. Birdi (Ed.), Handbook of Surface and Colloid Chemistry, CRC Press, New York, 2008 p, p. 197.
[35] S.E. Anachkov, S. Tcholakova, D.T. Dimitrova, N.D. Denkov, N. Subrahmaniam, P. Bhunia, Adsorption of linear alkyl benzene sulfonates on oil–water interface: effects of Na^+, Mg^{2+} and Ca^{2+} ions, Colloids Surf. A: Physicochem. Eng. Asp. 466 (2015) 18–27.
[36] F. Ravera, L. Liggieri, G. Loglio, Dilational rheology of adsorbed layers by oscillating drops and bubbles, in: R. Miller, L. Liggieri (Eds.), Interfacial Rheology, Brill, Leiden, 2009.
[37] S. Tcholakova, Z. Mitrinova, K. Golemanov, N. Denkov, M. Vethamuthu, K.P. Ananthapadmanabhan, Control of ostwald ripening by using surfactants with high surface modulus, Langmuir 27 (2011) 14807–14819.
[38] N.D. Denkov, S. Tcholakova, K. Golemanov, K.P. Ananthpadmanabhan, A. Lips, The role of surfactant type and bubble surface mobility in foam rheology, Soft Matter 5 (2009) 3389–3408.
[39] K. Golemanov, S. Tcholakova, N.D. Denkov, K.P. Ananthapadmanabhan, A. Lips, Breakup of bubbles and drops in steadily sheared foams and concentrated emulsions, Phys. Rev. E 78 (2008) 051405.
[40] P.A. Kralchevsky, K. Nagayama, Particles at Fluid Interfaces and Membranes: Attachment of Colloid Particles and Proteins to Interfaces and Formation of Two-Dimensional Arrays, Elsevier, Amsterdam, 2001.